Structure of the Amyloid-β (1−42) Monomer Absorbed To Model Phospholipid Bilayers: A Molecular Dynamics Study

Charles H. Davis[†] **and Max L. Berkowitz***[,‡]

Department of Biochemistry and Biophysics, University of North Carolina at Chapel Hill, Chapel Hill, North Carolina 27599, and Department of Chemistry, University of North Carolina at Chapel Hill, Chapel Hill, North Carolina 27599

Received: June 23, 2009; Revised Manuscript Received: September 10, 2009

The amyloid-β (Aβ) peptide, the 39 to 43 amino acid peptide that plays a substantial role in Alzheimer's disease, has been shown to interact strongly with lipids both in vitro and in vivo. Aβ−lipid interactions have been proposed as a considerable factor in accelerating Aβ aggregation through the templating role of membranes in aggregation disorders. Previous work has shown that anionic lipids are able to significantly increase Aβ aggregation rate and induce a structural conversion in Aβ from a random coil to a β-structure that is similar to the monomer structure observed in mature fibrils. However, it is unclear if this structural change occurs with the Aβ monomer because of direct interactions with the lipids or if the structural change results from protein−protein interactions during oligomerization. We use extensive replica exchange molecular dynamics simulations of an Aβ monomer bound to a homogeneous model zwitterionic or anionic lipid bilayer. From these simulations, we do not observe any significant β-structure formation except for a small, unstable β-hairpin formed on the anionic dioleylphosphatidylserine bilayer. Further, we see that the Asp23-Lys28 salt bridge that plays a role in β-hairpin formation is not substantially formed on the bilayer surface and that Lys28 preferentially interacts with lipids when bound to the bilayer. These results suggest that the structural conversion seen in experiments are not due to the ordering of monomeric Aβ on the bilayer surface but are a result of protein−protein interactions enhanced by Aβ binding to the cell membrane.

Introduction

The amyloid-β (Aβ) peptide is an amyloidogenic protein whose aggregation has been linked to neural degeneration[1−4] that is a hallmark of Alzheimer's disease. Because of the association of Aβ with Alzheimer's disease, Aβ has been extensively studied[1−4] over the past 20−30 years. In particular, the structure of the Aβ peptide, through its passage from monomer to small aggregate to fibril, has been a subject of great interest for both experimental[5−16] and computational[17−31] researchers. Knowledge of the structure of Aβ at each step of the aggregation pathway will provide insight into the mechanism of aggregation that can hopefully be exploited for therapeutic benefits. Previous research has already made significant progress on this front as the dogma of Aβ neurotoxicity has been shifting away from mature fibrils and toward small oligomers as one of the main neurotoxic species in Alzheimer's disease.[5,6,32] This knowledge places even further impact on gaining a fundamental understanding of the earliest stages of Aβ aggregation as a major target for prevention of extensive neurodegeneration.

While it is clear that the first stages of Aβ aggregation are vital to the progress of Alzheimer's disease, it has not yet been determined exactly what factors influence this initial conversion from monomer to oligomer. While oligomerization does occur naturally in solution, there are other possible factors that may catalyze this reaction. Recent work[5−16] has demonstrated that cell membranes may play a significant catalytic role in increasing Aβ aggregation rates. The Aβ peptide is derived from the transmembrane amyloid precursor protein (APP).[1−3] Upon cleavage from APP, the C-terminus[1−3] of Aβ maintains a significant portion of the transmembrane region of APP. Extensive experimental work[5−12] has shown that Aβ, when mixed with lipid vesicles of various structure and headgroup charge, will aggregate at a much faster rate then in solution. Further results have demonstrated that this interaction between Aβ and lipids will induce a structural conversion[5−16] from a disordered peptide into a peptide dominated by β-structure. Mixing Aβ peptide with anionic lipids, in the form of vesicles or bilayers, has shown a substantial increase in both aggregation rate and secondary structure formation.[5,9−12,14−16] Also, it has been shown that extensive interactions with cell membranes can lead to substantial pore formation and disruption of ion balance[13,33] across the bilayer, which may play a role in Aβ neurotoxicity.

While experimental results have demonstrated an extensive interaction of Aβ with lipid bilayers, these same experimental techniques are limited in resolution. Circular dichroism, nuclear magnetic resonance, electron microscopy; and other common techniques[6−16] require a low concentration to study Aβ without immediate aggregation, which prevents these techniques from being able distinguish if Aβ is in a monomeric or small oligmeric state. This subtle shortcoming due to the nature of Aβ does cloud one aspect of these results: Is the secondary structure change observed in experiment inherent to the Aβ monomer or does the structural conversion occur due to peptide−peptide interactions that are enhanced on the lipid surface? Thus, molecular dynamics (MD) simulations would be ideal for determining the structure of Aβ as a monomer on an atomic level.

* Corresponding author: Phone: 919-962-1218; fax: 919-962-2388; e-mail: maxb@unc.edu.
[†] Department of Biochemistry and Biophysics.
[‡] Department of Chemistry.

10.1021/jp905889z CCC: $40.75
Published on Web 10/06/2009

MD simulations have been extensively performed on the Aβ peptide. Simulations on the full length monomer,[20,22,23,30,31] on monomer fragments,[19,24−26,28] on small oligomers[17,21,24,29] and on full fibrils[27] using all atom[17−23,25−31] or coarse grain techniques[24,29] in both explicit[18,19,22,23,25−31] and implicit[17,20,21,24] solvent have produced significant insight into the structure of Aβ at each step of aggregation. Replica exchange MD simulations,[17−22] which allow for much more extensive motion of the peptide through its configurational space by effectively overcoming barriers on the conformational free energy surface, have been particularly insightful for Aβ structure studies. These replica exchange studies[17−22] on Aβ have shown that the peptide does have a predominantly random coil structure in solution but can still form some stable secondary structure, such as β-hairpins or small helices, that may help to accelerate aggregation. However, these same studies have not yet been extended to Aβ in an explicit membrane environment. Previous studies have investigated the stability of a preinserted[30,31] Aβ into either an explicit or implicit membrane environment, but these works did not concentrate on Aβ structure when bound to the membrane surface. A previous work of ours[34] investigated Aβ binding free energies to various bilayers of differing headgroup charge, but we did not investigate Aβ structure because of lack of sampling without replica exchange. In this work, we use the replica exchange method to study Aβ structure and the effect of both peptide charge and lipid charge on peptide structure. As anionic lipids bilayers are able to decrease local pH,[9,35] it is necessary to study the effect of lipid binding on Aβ with different total charges. The results of this work will help to elucidate the mechanism of structural change experimentally observed in Aβ aggregation at a molecular level not available to many current experimental techniques.

Theoretical Methods

Initial Conditions. The initial structures used for replica exchange simulations were obtained from a previous work[34] by our group. In that work, a random coil structure of the 42 amino acid Aβ peptide was systematically pulled to the surface of an equilibrated 128 lipid dipalmitoylphosphatidylcholine (DPPC) or dioleylphosphatidylserine (DOPS) bilayer using the umbrella sampling technique, and a free energy of binding was calculated. The initial conditions for the replica exchange simulations presented here were obtained from the final snapshots of MD simulations at the bound free energy minimum, as determined from the calculated free energy profiles for binding. These final snapshots from the simulations occurred at an Aβ-bilayer center-of-mass separation of 2.1 nm with DPPC and 2.4 nm with DOPS. Thus, the initial structures chosen for the replica exchange simulations described here represent configurations where the 80 ns of restrained MD simulations allowed for extensive simulation time to equilibrate the Aβ-bilayer system. The Aβ-bilayer center-of-mass restraint used in the previous work was removed for replica exchange, ensuring that the Aβ was not restrained to the bilayer surface.

Peptide and Lipid Parameters. Replica exchange simulations were performed using the GROMACS 4.0 simulation package.[36−39] The Aβ peptide was described using the united-atom GROMOS96 force field.[36−38] The DPPC and DOPS lipids were described using the Berger[40] force field parameters. These force fields were chosen to match our previous work[34] and because of the extensive use of each force field in previous molecular dynamics studies. The system was solvated with SPC/E model[41] water and included counterion and co-ion Na^+/Cl^- salt. As the local pH near anionic lipid bilayers is lower than bulk,[9,35] it was important to perform these simulations at physiological pH and also at a lower pH to determine if peptide protonation state could affect Aβ structure near lipids. Thus, simulations were performed with Aβ at a −3 total charge, which is the physiological charge of Aβ, and with a net 0 total charge due to protonation of three histidine residues. This 0 total charge state would be a close approximation of the charge on Aβ at pH 5, which is a feasible pH for Aβ bound to an anionic bilayer surface. Therefore, the −3 total charge simulations are termed the pH 7 simulations and the 0 total charge simulations are termed the pH 5 simulations throughout, for simplicity. The N-terminus was represented by NH_3^+, and the C-terminus was represented by COO^- to match the most likely charge state at physiological pH. Thus, four total replica exchange simulations are performed with two peptide charge states on either a DPPC or DOPS bilayer. Exact contents of the simulations are given in the Supporting Information (Table S1). For each replica, temperature was held constant using a Nose−Hoover[42] scheme with a relaxation time of 0.5 ps under constant volume (NVT) conditions. All bonds were constrained using the LINCS algorithm,[43] which allowed for a time step of 3 fs. Long range electrostatic contributions were maintained using the SPME algorithm[44] with periodic boundary conditions in all three dimensions. Secondary structure was calculated using the DSSP algorithm[45] within GROMACS and all other analysis was performed using GROMACS utilities. As a clarification note for the tables and figures, a discontinuous trajectory refers to a system trajectory obtained at a fixed temperature during the replica exchange, while a continuous trajectory refers to a trajectory obtained by reordering the set of discontinuous trajectories so that one initial structure is followed through the temperature space during the full simulation time.

Replica Exchange Details. The temperature exchange simulations involved 83 replicas spaced between 325 K and 502 K. The exact temperatures of all replicas are provided in the Supporting Information (Table S2). The temperatures were chosen using the temperature generator for REMD-simulations[46] associated with the GROMACS package. Thus, 80 ns (pH 7) or 110 ns (pH 5) molecular dynamics simulations were performed for each of the 83 replicas at random initial velocities with exchanges attempted every 3 ps and coordinates written every attempted exchange. The pH 5 simulations were extended to 110 ns to determine the stability of secondary structure formed at the end of the 80 ns simulation. With a minimum of 80 ns total simulation time and 3 ps exchanges, over 26 000 exchange attempts are made during the span of the simulation. Further, results from the simulations showed an exchange probability of 0.2−0.35 over all temperatures. The combination of a rate of exchange greater than 1 ps and over 20 000 exchange attempts should guarantee at least one full transit for the replicas through the temperature space and, subsequently, a well-mixed[47] replica exchange simulation. All details involving the replica exchange and the replica temperatures were the same for the four initial conditions.

Bilayer Constraint. At the high temperatures used in this simulation, neither the DPPC or DOPS bilayer was stable. Thus, a restraint was necessary to keep the fidelity of the bilayer while still allowing the peptide significant conformational flexibility. Further, it was important to maintain individual lipid flexibility within the bilayer as lipid−protein interactions may play a significant role in Aβ structure. A restraint was chosen to keep the average separation along the *Z*-axis between the phosphate groups of the two leaflets of the bilayer constant. In order to impose this restraint, the 64 phosphate atoms from each leaflet

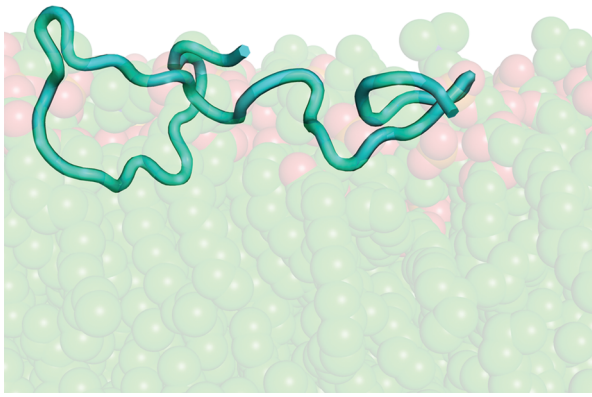

Figure 1. Initial structure of pH 7 Aβ peptide on DPPC bilayer. Solvent and ions were removed for clarity.

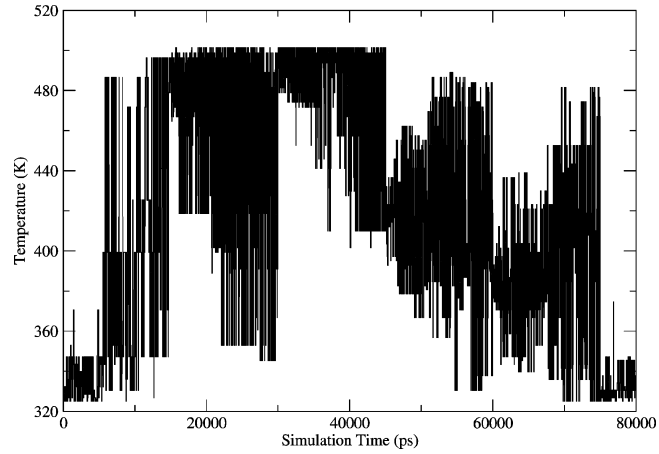

Figure 2. Time series of temperature exchange for replica starting at 325 K for the pH 7 Aβ peptide on a DPPC bilayer.

were grouped together and a harmonic constraint was applied to the average distance along the *Z*-axis between the center-of-mass of these two groups. By imposing the constraint on the center-of-mass separations of the group instead of each phosphate individually, it allows for each lipid to fluctuate significantly as long as the average *Z* value for each leaflet remains relatively constant. To calculate the average constraint distance for the DPPC and DOPS bilayers, we used the final 20 ns of the umbrella sampling simulations of our previous work.[34] From these previous simulations, we calculated that the average phosphate−phosphate distance on DPPC was 3.90 nm and the average distance on DOPS was 4.16 nm. It was necessary to impose a force constant of 4 kJ/(mol nm^2) to prevent the bilayer from breaking apart and to prevent exceptional amounts of water from penetrating the bilayer. Visual inspection of the trajectories at 502 K show that the bilayer remains together throughout the 80 ns simulation and the extent of bilayer fluctuations are not significantly different in comparison to the simulation at 325 K. Further, we calculated the number of water molecules that interact with the hydrophobic core of the bilayer. At 502 K, the number of water molecules interacting with the bilayer core is three times larger than the number of water molecules interacting with the bilayer core at 325 K, and these quantities are stable over the length of the simulation. Both the leaflet to leaflet restraint and the constant volume (NVT) simulation condition, which also acts as a restraint on the system, prevent the increase in water molecules near the hydrophobic core at high temperature from disrupting the bilayer structure, thus forcing more water molecules into the hydrophobic core and eventually dissolving the bilayer. As previously mentioned, the leaflet to leaflet restraint on the bilayer was the only specific restraint applied on the system, and the peptide was not restrained to the bilayer surface during replica exchange.

Results

Aβ-Bilayer Replica Exchange MD Setup. In order to properly assess the structure of monomeric Aβ at the surface of the bilayer, replica exchange simulations were performed for the 42 amino acid form of the Aβ peptide at pH 7 (−3 total charge) or pH 5 (0 total charge) on either a homogeneous DPPC or DOPS bilayer. The initial structures for each of the four replica exchange simulations were taken as the final equilibrated structures at the membrane-bound free energy mimima determined in a previous work.[34] Figure 1 is a representative example of one of the initial configurations for Aβ bound to the bilayer surface. The initial configurations for Aβ represent an Aβ structure where the peptide is strongly bound to the interfacial region of the bilayer with some amino acid side chains inserted into the bilayer hydrophobic core and some side chains either fully solvent exposed or interacting with the lipid headgroups.

MD simulations using the replica exchange methodology were then performed using these four initial configurations over a temperature range of 325 K to 502 K. As demonstrated in Figure 2, the replica exchange setup employed in this work allows each replica to adequately explore the temperature space during the duration of the simulation, which was consistent over all four simulation conditions. In combination with the 3 ps exchange rate of these simulations, the extensive motion through the temperature space should allow these replica exchange simulations to be considered well mixed and the local configurational space well sampled.[47] Further analysis at the lowest temperature (325 K) should provide an appropriate estimate to the conformational space of Aβ while bound to a bilayer surface. The use of a weak restraint between the average positions of the phosphate groups from each leaflet of the bilayer allows for some natural fluctuations of the bilayer surface without allowing the bilayer to dissolve. Allowing the bilayer to be more flexible may play a significant role in the dynamics of a protein bound to the bilayer surface.

Aβ Secondary Structure on the Bilayer Surface. Secondary structure content of the protein was calculated at 325 K for all four systems as a means of determining how the membrane surface influences Aβ structure (Figure 3). From these calculations, it is clear that Aβ remains in a predominantly random coil configuration throughout the duration of the simulation. In particular, at pH 7, the protein contains almost no ordered structure except for a small amount of β-sheet formed near the end of the simulation of pH 7 Aβ on DOPS. However, at pH 5, Aβ is able to adopt structures containing more ordered secondary structure. Most notably, the pH 5 protein on DOPS develops a turn/β-sheet structure from residues 21−34 beginning at 76 ns of the simulation, which can be seen more clearly in Figure 4A. This structure is reminiscent of a β-hairpin, which has been postulated to be the building block[48,49] of Aβ fibrils. On DPPC, it appears that a similar structure is formed, also at 75 ns, but this structure spans fewer residues and is more transient. The replica exchange simulations at pH 5 on DPPC and DOPS were both extended 30 ns to test the hairpin stability. From Figure 3, it is obvious that this structure is still not stable over the length of the simulation and has quickly disappeared after 86 ns of total simulation time. This β-hairpin structure only appears for 10 ns of the 110 ns of total simulation time and does not significantly influence the average structure of the peptide during

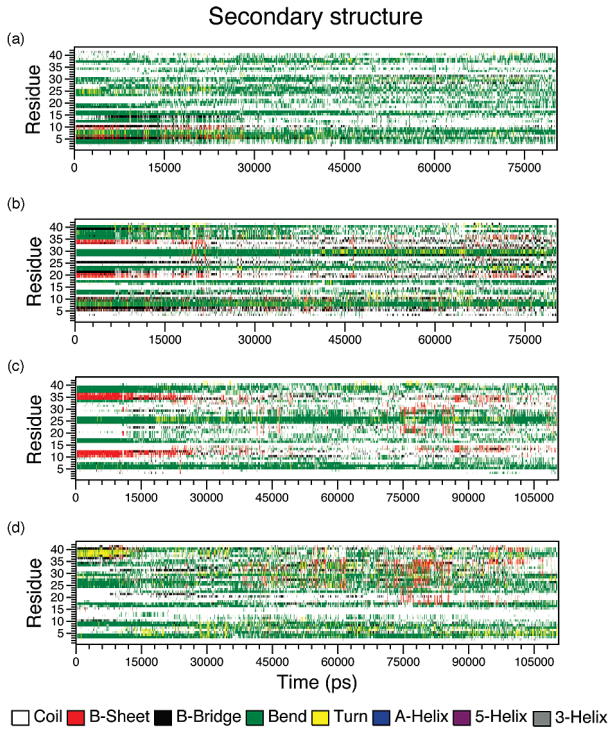

Figure 3. Secondary structure for each residue at 325 K for the discontinuous simulations of (a) pH 7 Aβ on the DPPC bilayer, (b) pH 7 Aβ on DOPS bilayer, (c) pH 5 Aβ on the DPPC bilayer, and (d) pH 5 Aβ on the DOPS bilayer. The secondary structure calculations are for the full 80 ns simulations for pH 7 Aβ and the full 110 ns for pH 5 Aβ. Secondary structure readout was produced using DSSP within GROMACS.

simulation. Finally, a turn and some β-sheet structure are transiently formed in the last five residues of the pH 5 Aβ during the simulation on DOPS. This small turn has been previously seen[22] in studies of Aβ, due to Gly37 and Gly38 which have been predicted to strongly favor formation of turns. These replica exchange simulations confirm that this turn is feasible, yet it is not stable in the interfacial membrane environment.

Asp23-Lys28 Salt Bridge Stability. The salt bridge that can be formed between Asp23 and Lys28 has previously been implicated[19,25,26,48,50] to be a major factor in fibril formation by Aβ and has been observed in structures of Aβ fibrils.[48] A recent experimental work[50] has demonstrated that a covalent lactam bridge created between Asp23 and Lys28 substantially increases the Aβ aggregation rate. Further, many computational studies[19,25,26] have shown that this salt bridge is significant in the formation of a β-hairpin in monomeric Aβ. However, it is still a point of contention if this salt bridge is necessary for fibril-like β-sheet formation in Aβ or if hydrophobic interactions drive this sheet formation and the salt bridge is a secondary effect of β-sheet formation. To understand the properties of the salt bridge in our system, we calculated the distance between the C_γ group of Asp23 and the N_ξ group of Lys28 during the pH 5 Aβ replica exchange simulations at 325 K from 75 ns to 81 ns on the DOPS bilayer, where the hairpin is transiently stable (Figure 4A). Salt bridges between these two residues have previously[19] been described as close-contact salt bridges for separations less than 4.5 Å and mediated salt bridges for separations within 4.5 Å to 7 Å. The snapshots shown in Figure 4B and the $N_\xi - C_\gamma$ distance plot in Figure 4C demonstrate that Aβ tends to adopt one of two structures depending on the Asp23-Lys28 distance. When Asp23 and Lys28 are separated by a significant distance (labeled (1) in the figure), Aβ adopts a β-hairpin structure with a turn between residues 21−24 (Ala-Glu-Asp-Val). However, when a mediated salt bridge is formed between Asp23 and Lys28 (labeled (2) in the figure), the turn is shifted from residues 21−24 to approximately residues 18−22 (Val-Phe-Phe-Ala-Glu) and a new, smaller turn is created between Asp23 and Lys28 to accommodate this salt bridge formation. From Figure 4C, Aβ appears to fluctuate between these two strand-loop-strand structures over the time period studied and that neither structure appears to be significantly more stable then the other. Further, no close-contact salt bridges appear to be formed between Asp23 and Lys28, in contrast to simulations[19] performed in solution that investigated this salt-bridge formation. It is important to note that these ordered β-structures were not significantly stable over the full simulation time and were only formed with the pH 5 peptide interacting with either bilayer.

Aβ Distribution on the Bilayer Surface. While the secondary structure and salt-bridge calculations did not show a significant difference between Aβ structure on the DPPC versus DOPS bilayers, we also performed density distribution calculations to determine if regions of the Aβ peptide interacted differently with the zwitterionic or anionic lipids. For this analysis, Aβ was separated into a charged section (residues 1−23) and a hydrophobic section (residues 24−42) to see how the peptide interacted with the charged headgroups on the bilayer surface. In Figure 5, the left panel shows the pH 5 Aβ density distribution on DPPC. This plot shows that both the hydrophobic and charged sections of Aβ are interacting with the interfacial region of the bilayer. Further, the density of the phosphate atoms in DPPC is also shown, which further supports an interfacial distribution for the peptide. The charged and hydrophobic sections of the peptide appear to be distributed very similarly, both in the peak location and the width of the distribution. It also appears that the hydrophobic section of the peptide is not significantly inserted into the bilayer core. For the distribution on the DOPS bilayer given on the right panel of Figure 5, a similar pattern is observed. Both sections of the peptide appear to be sitting in the interfacial region of the bilayer, and the distributions from both the charged and hydrophobic sections overlap. However, one significant difference is that the hydrophobic section of the peptide appears to have a broader distribution on DOPS, including significant tails on both sides of the distribution indicating either partial insertion of the hydrophobic section into the bilayer core or more solvent exposure of the hydrophobic residues at the C-terminus. Further, the charged section of the peptide also is able to become significantly solvent exposed by being distributed outside of the DOPS density, which is not seen in the DPPC bilayer. Thus, while Aβ on the DPPC bilayer has an almost parallel arrangement with both sections of the peptide bound to the interfacial region of the bilayer, Aβ bound to DOPS is able to adopt a larger range of distributions on the bilayer surface, including a distribution with a more exposed hydrophobic C-terminus, which may play a significant role in peptide−peptide interactions that drive aggregation.

Finally, we investigated the distribution of various amino acids on Aβ with respect to the bilayer. In particular, we looked at Lys28, which has been shown to be integral to bilayer association,[12,16,33] as well as its importance in the Asp23-Lys28 salt bridge described previously. As shown in Figure 5, Lys28 tends to distribute on the interfacial region of the bilayer near the hydrophobic core, independent of the charge of the lipids. Interestingly, while the Lys28 density does overlap somewhat with the phosphate density from the lipid headgroups, the lack

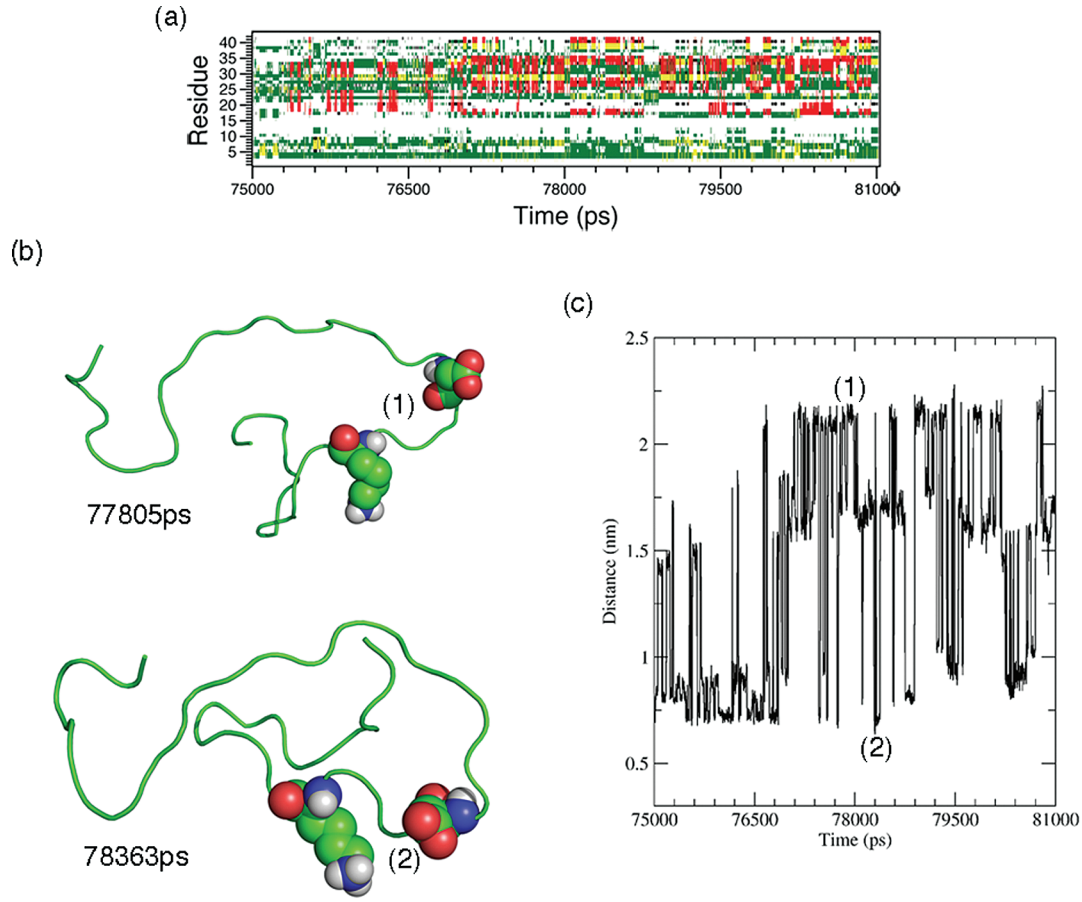

Figure 4. (a) Secondary structure for pH 5 Aβ on the DOPS bilayer for the discontinuous simulations at 325 K from 75 ns to 81 ns of simulation time. (b) Aβ structure at time points of 77.805 ns and 78.363 ns showing the average protein structure. Residues Asp23 and Lys28 are shown in space filling mode. (1) and (2) on the snapshots are labels for the salt bridge that could be formed between these residues. (c) Plot of the distance between the C_γ of Asp23 and N_ξ of Lys28 over simulation from 75 ns to 81 ns. The labels (1) and (2) on the plot represent the Asp−Lys distance shown in the snapshots from (b).

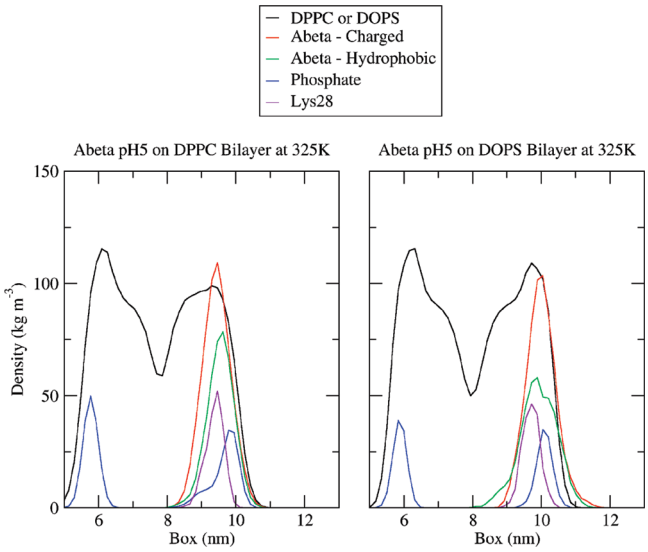

Figure 5. Density distribution of Aβ on DPPC or DOPS bilayer at 325 K. The Abeta-charged density distribution represents residues 1−23 of the Aβ peptide while the Abeta-hydrophobic density distribution represents residues 24−42. The phosphate density distribution represents the distribution of phosphate atoms on the individual DPPC or DOPS lipids within the bilayer.

of complete overlap and different density peaks for Lys28 and the lipid phosphate atoms demonstrates that Lys28 is likely not bonding strongly to these atoms throughout the entirety of the simulation. Further, the Lys28 distribution near the lower end of the Aβ hydrophobic density distribution indicates that Lys28 may be playing a role in anchoring the peptide to the interfacial region of the bilayer through interactions with the glycerol backbone or hydrophobic tails of the lipids. These results of the Lys28 density distribution studies are evidence that the role of Lys28 in Aβ interactions with the bilayer surface is to stabilize the interaction of Aβ with the interfacial region of the bilayer, thus contributing to the strong binding free energies predicted[34] for Aβ binding to either the DPPC or DOPS bilayer surface.

Discussion

The results of the replica exchange simulations of the Aβ 1−42 peptide on the zwitterionic DPPC or anionic DOPS bilayer surface provides insight into the structure of the monomeric peptide when bound to a membrane. These simulations appear to be well-mixed replica exchange simulations, and the weak restraints applied to prevent the bilayer from dissolving at high temperature allow for significant bilayer motion, which may influence peptide structure or distribution on the bilayer surface. Bilayer restraints were also used in a previous all-atom replica exchange study[51] with a peptide-bilayer system, although those restraints were much more constricting since the temperatures used in the replica exchange simulations were over a much larger range (350 K to 800 K).

The secondary structure results from these simulations show that, even when bound to the bilayer surface, monomeric Aβ

does not adopt a stable secondary structure. Many replica exchange simulations[17−22] have previously been performed using full-length[20,22] Aβ or Aβ fragments[18,19] in both explicit and implicit solvent. These studies[17−22] have shown that Aβ prefers a random coil structure in solution, but it is able to form stable secondary structure, which can range from strand-loop-strand structures to small helices, for times during the simulation. One of the most important aspects of these previous studies is that Aβ is able to adopt a multitude of structures and is a highly flexible peptide in solution, which is considered an important aspect of Aβ aggregation, over time scales comparable to the simulations performed in this work. However, our results indicate that the interactions of Aβ with the lipid bilayer do not promote structural ordering similar to observations made in aqueous solution and that conformational motion is likely restricted because of direct protein−lipid interactions. At pH 7, Aβ does not form any stable secondary structure on either bilayer, while at pH 5, Aβ is able to form some transient β-hairpin structure, especially when bound to the DOPS bilayer. Further, our results show that different β-hairpin structures are formed when bound to DOPS, and the Asp23−Lys28 salt bridge interaction may play a significant role in determining which structure is stabilized. These results may appear contrary to experimental results[5,9−12] showing a significant increase in β-structure when Aβ is mixed with anionic lipid vesicles. It is important to note that those studies are not able to distinguish between Aβ monomers and small Aβ oligomers on the lipid surface, and our results imply that the β-structure seen in experiment is due to peptide−peptide interactions that occur during oligomerization, which are promoted when Aβ is bound to the anionic lipid surface.

The results from the Aβ density distribution analysis also illustrate important aspects of Aβ interactions with lipid bilayers. The density distributions show that the peptide interacts strongly with the interfacial region of the bilayer. Further, residues such as Lys28, when not engaging in intrapeptide salt bridge interactions, are likely interacting with the glycerol backbone or carbon tails of lipid molecules, which stabilizes this binding. The extent of contact between the bilayer surface and Aβ was also calculated at the extreme of the replica exchange simulation, 502 K (Figure S3). Even at 502 K, at least 25 of the 42 residues of Aβ maintain strong contact with the bilayer surface and, on average, greater than 35 residues remain in contact, independent of bilayer or peptide charge. These results are not surprising in light of our previous calculations of significant binding free energies for Aβ to the bilayer surface, which are substantially larger than kT even at a system temperature of 502 K. These results also agree with previous molecular dynamics studies of preinserted Aβ which show either partial or full removal of a transmembrane Aβ from a DPPC bilayer over simulation time because of favorable interactions of Aβ with the interfacial region[30,31,34] of the bilayer. Further, previous experimental work[7] has observed favorable interactions of Aβ with the interfacial region of the bilayer both in full length Aβ and Aβ fragments.

The results of these replica exchange molecular dynamics simulations provide significant insight toward the role of cell membranes in Aβ aggregation. While the bilayers used in this study are only simplified models of the complex lipid and cholesterol mixtures of which cellular membranes are composed, these model bilayers do provide an appropriate system for testing Aβ-bilayer interactions on the atomic levels available to molecular dynamics simulations. Further, even though the replica exchange techniques used in this work do improve upon sampling of the conformational free energy surface of Aβ when bound to the bilayer, there are still limitations to the ability of MD to overcome significant free energy barriers over the course of a simulation. Nevertheless, in comparison to previous replica exchange simulations[17−22] of the Aβ peptide in solution with similar temperature ranges and time scales that show significant peptide flexibility, the motion of the Aβ peptide is severely retarded when bound to the bilayer surface. This comparison between similar replica exchange studies of Aβ in solution and on the bilayer surface implies that Aβ interactions with the bilayer surface substantially affect Aβ dynamics in comparison to Aβ dynamics in solution.

Further, the results of this work imply that the role of the bilayer in Aβ aggregation may be multifold, as has been previously postulated.[5,6,52] First, because of the strong binding of Aβ to the bilayer surface, Aβ peptides will accumulate on the surface of the bilayer. This will transiently increase local peptide concentration and increase diffusion by limiting motion to two dimensions, which will speed up aggregation in comparison to aggregation rates in solution. Next, when bound to the anionic bilayer, the local pH will drop. As has been observed in vitro, Aβ aggregation rates increase in solution at lower pH[53] and the same pattern may hold on the bilayer surface. Finally, the results imply that the hydrophobic section of Aβ is more exposed and accessible on the bilayer surface, which will promote protein−protein interactions through mutual hydrophobic regions of adjacent Aβ monomers that will drive the earliest stages of aggregation. However, these results do not observe any significant structure formation of the monomeric Aβ peptide on the surface of the bilayer, which had been postulated as playing a role in the increased aggregation rate due to lipid interactions. Our results predict that the strongly promoted secondary structure formation in Aβ when mixed with lipids observed in experiment is likely due to the peptide−peptide interactions that are greatly enhanced by interactions with the bilayer. Thus, experimental studies using highly precise methods for determining Aβ structure both in monomer and small oligomer (dimer, trimer, tetramer) form when bound to a lipid surface will be necessary to determine where the secondary structure formation observed previously is originating. Further, future all-atom or coarse-grain MD studies using a similar replica exchange setup employed in this work with multiple Aβ peptides bound to a bilayer in which direct peptide−peptide interactions and potential secondary structure change are followed would also be very insightful for determining if protein−protein interactions are the cause of the secondary structure change seen in experiment during Aβ aggregation near a membrane surface.

Conclusions

In this work, replica exchange MD simulations were performed on all-atom representations of the 42 amino acid Aβ on model lipid bilayers using novel restraints to maintain bilayer integrity at high temperatures. The replica exchange simulations appear to be well mixed and allow for significant conformational freedom for the peptide on the bilayer surface in comparison to MD simulations previously performed at 323 K.[34] The results of these simulations show that no stable secondary structure is formed by the Aβ monomer at either pH 7 or pH 5 when bound to the homogeneous DPPC or DOPS bilayers. A salt bridge between Asp23 and Lys28, which may play a significant role in Aβ aggregation, is formed on the DOPS bilayer when the peptide has a net neutral charge, and the formation of the salt bridge imposes a β-hairpin like structure on the peptide. However, this salt bridge is not stable and this secondary

structure is not maintained because of the extensive peptide−lipid interactions that are precluding the intrapeptide interactions necessary for stable secondary structure. In particular, Lys28 substantially interacts with the phosphate moiety and glycerol backbone of the lipid, which stabilizes protein binding to the lipid even at 502 K. It appears, from these results, that the strong lipid−protein interactions which force the tight binding of Aβ to the bilayer surface also prevent the internal interactions which would promote the secondary structure change observed during Aβ aggregation in experiment.

The results of this work raise interesting questions regarding the earliest stages of Aβ aggregation near the bilayer surface. Experimental techniques have observed significant β-structure formation when Aβ is incubated with anionic lipid. Our observations tend to indicate that this β-structure formation is not due to structuring at a monomer level but is potentially due to peptide−peptide interactions that are enhanced on the bilayer surface. Further, the lack of secondary structure for monomeric Aβ bound to the bilayer surface may also shed some insight into the large diversity of oligomers that have been observed during Aβ aggregation. As the Aβ monomer is more extended in its membrane-bound, unstructured form, aggregation on the bilayer surface may lead to oligomer structures that are less compact then oligomers observed in solution. In the least, oligomers formed on the bilayer surface should be less structured than oligomers in solution that are forced to have a more compact, ordered structure due to interactions with water. Our work demonstrates that interactions with a membrane significantly affects structural dynamics of the Aβ monomer in comparison to Aβ in solution, which may in turn considerably alter the pathway of Aβ aggregation near the cell membrane.

Acknowledgment. This work was supported by the National Science Foundation under grant number MCB-0615469. The authors thank Z. Zhang for technical assistance on molecular dynamics simulations, and the UNC Research Computing Group for providing and maintaining the computing resources used in this work.

Supporting Information Available: Table S1 lists the full contents of all of the replica exchange simulations performed. Table S2 lists the temperatures used for replica exchange. Figure S3 provides plots of contact score over time for the discontinuous simulations at 502 K. This material is available free of charge via the Internet at http://pubs.acs.org.

References and Notes

(1) Kang, J.; Lemaire, H.-G.; Unterbeck, A.; Salbaum, J. M.; Masters, C. L.; Grzeschik, K.-H.; Multhaup, G.; Beyreuther, K.; Müller-Hill, B. *Nature* **1987**, *325*, 733.
(2) Miller, D. L.; Papayannopoulos, I. A.; Styles, J.; Bobin, S. A.; Lin, Y. Y.; Biemann, K.; Iqbal, K. *Arch. Biochem. Biophys.* **1993**, *301*, 41.
(3) Selkoe, D. J. *Physiol. Rev.* **2001**, *81*, 741.
(4) Shankar, G. M. *Nat. Med.* **2008**, *14*, 837.
(5) Matsuzaki, K. *Biochim. Biophys. Acta* **2007**, *1768*, 1935.
(6) Aisenbery, C.; Borowik, T.; Byström, R.; Bokvist, M.; Lindström, F.; Misiak, H.; Sani, M. A.; Gröbner, G. *Eur. Biophys. J.* **2008**, *37*, 247.
(7) Yip, C. M.; McLaurin, J. *Biophys. J.* **2001**, *80*, 1359.
(8) Yoda, M.; Miura, T.; Takeuchi, H. *Biochem. Biophys. Res. Commun.* **2008**, *376*, 56.
(9) Terzi, E.; Hölzemann, G.; Seelig, J. *J. Mol. Biol.* **1995**, *252*, 633.
(10) McLaurin, J.; Chakrabartty, A. *Eur. J. Biochem.* **1997**, *245*, 355.
(11) Ege, C.; Majewski, J.; Wu, G.; Kjaer, K.; Lee, K. Y. C. *ChemPhysChem.* **2005**, *6*, 226.
(12) Bokvist, M.; Lindström, F.; Watts, A.; Gröbner, G. *J. Mol. Biol.* **2004**, *335*, 1039.
(13) Ambroggio, E. E.; Kim, D. H.; Separovic, F.; Barrow, C. J.; Barrow, C. J.; Barnham, K. J.; Bagatolli, L. A.; Fidelio, G. D. *Biophys. J.* **2005**, *88*, 2706.
(14) Wong, P.; Schauerte, J. A.; Wisser, K. C.; Ding, H.; Lee, E. L.; Steel, D. G.; Gafni, A. *J. Mol. Biol.* **2009**, *386*, 81.
(15) Dante, S.; Hauss, T.; Dencher, N. A. *Biophys. J.* **2002**, *83*, 2610.
(16) Chauhan, A.; Ray, I.; Chauhan, V. P. S. *Neurochem. Res.* **2000**, *25*, 423.
(17) Anand, P.; Nandel, F. S.; Hansmann, U. H. E. *J. Chem. Phys.* **2008**, *128*, 165102.
(18) Wu, C.; Murray, M. M.; Bernstein, S. L.; Condron, M. M.; Bitan, G.; Shea, J. E.; Bowers, M. T. *J. Mol. Biol.* **2009**, *387*, 492.
(19) Baumketner, A.; Shea, J. E. *J. Mol. Biol.* **2007**, *366*, 275.
(20) Yang, M.; Teplow, D. B. *J. Mol. Biol.* **2008**, *384*, 450.
(21) Jang, S.; Shin, S. *J. Phys. Chem. B* **2008**, *112*, 3479.
(22) Sgourakis, N. K.; Yan, Y.; McCallum, S. A.; Wang, C.; Garcia, A. E. *J. Mol. Biol.* **2007**, *368*, 1448.
(23) Tomaselli, S.; Esposito, V.; Vangone, P.; van Nuland, N. A. J.; Bonvin, A. M. J. J.; Guerrini, R.; Tancredi, T.; Temussi, P. A.; Picone, D. *ChemBioChem* **2006**, *7*, 257.
(24) Dong, X.; Chen, W.; Mousseau, N.; Derreumaux, P. *J. Chem. Phys.* **2008**, *128*, 125108.
(25) Reddy, G.; Straub, J. E.; Thirumalai, D. *J. Phys. Chem. B* **2009**, *113*, 1162.
(26) Tarus, B.; Straub, J. E.; Thirumalai, D. *J. Am. Chem. Soc.* **2006**, *128*, 16159.
(27) Buchete, N.-V.; Tycko, R.; Hummer, G. *J. Mol. Biol.* **2005**, *353*, 804.
(28) Cruz, L.; Urbanc, B.; Borreguero, J. M.; Lazo, N. D.; Teplow, D. B.; Stanley, H. E. *Proc. Natl. Acad. Sci. U.S.A.* **2005**, *102*, 18258.
(29) Urbanc, B.; Cruz, L.; Ding, F.; Sammond, D.; Khare, S.; Buldyrev, S. V.; Stanley, H. E.; Dokholyan, N. V. *Biophys. J.* **2004**, *87*, 2310.
(30) Xu, Y.; Shen, J. J.; Luo, X. M.; Zhu, W. L.; Chen, K. X.; Ma, J. P.; Jiang, H. L. *Proc. Natl. Acad. Sci. U.S.A.* **2005**, *102*, 5403.
(31) Lemkul, J. A.; Bevan, D. R. *Arch. Biochem. Biophys.* **2008**, *470*, 54.
(32) Klein, W. L.; Stine, W. B.; Teplow, D. B. *Neurobiol. Aging* **2004**, *25*, 569.
(33) Arispe, N.; Diaz, J. C.; Simakova, O. *Bioch. Biophys. Acta* **2007**, *1768*, 1952.
(34) Davis, C. H.; Berkowitz, M. L. *Biophys. J.* **2009**, *96*, 785.
(35) Van Klompenburg, W.; de Kruijff, B. *J. Membr. Biol.* **1998**, *162*, 1.
(36) Hess, B.; Kutzner, C.; van der Spoel, D.; Lindahl, E. *J. Chem. Theory. Comput.* **2008**, *4*, 435.
(37) Van der Spoel, D.; Lindahl, E.; Hess, B.; Groenhof, G.; Mark, A. E.; Berendsen, H. J. C. *J. Comput. Chem.* **2005**, *26*, 1701.
(38) Lindahl, E.; Hess, B.; van der Spoel, D. *Comput. Phys. Commun.* **1995**, *91*, 43.
(39) Hukushima, K.; Nemoto, K. *J. Phys. Soc. Jpn.* **1996**, *65*, 1604.
(40) Berger, O.; Edholm, O.; Jahnig, F. *Biophys. J.* **1997**, *72*, 2002.
(41) Berendsen, H. J. C.; Grigera, J. R.; Straatsma, T. P. *J. Phys. Chem.* **1987**, *91*, 6269.
(42) Nosé, S. J. *J. Chem. Phys.* **1984**, *81*, 511.
(43) Hess, B. *J. Chem. Theory Comput.* **2008**, *4*, 116.
(44) Essman, U.; Perera, L.; Berkowitz, M. L.; Darden, T.; Lee, H.; Pedersen, L. G. *J. Chem. Phys.* **1995**, *103*, 8577.
(45) Kabsch, W.; Sander, C. *Biopolymers* **1983**, *22*, 2577.
(46) Patriksson, A.; van der Spoel, D. *Phys. Chem. Chem. Phys.* **2008**, *10*, 2073.
(47) Abraham, M. J.; Gready, J. E. *J. Chem. Theory Comput.* **2008**, *4*, 1119.
(48) Petkova, A. T.; Ishii, Y.; Balbach, J. J.; Antzutkin, O. N.; Leapman, R. D.; Delaglio, F.; Tycko, R. *Proc. Natl. Acad. Sci. U.S.A.* **2002**, *99*, 16742.
(49) Petkova, A. T.; Yau, W. M.; Tycko, R. *Biochemistry* **2006**, *45*, 498.
(50) Sciarretta, K. L.; Gordon, D. J.; Petkova, A. T.; Tycko, R.; Meredith, S. C. *Biochemistry* **2005**, *44*, 6003.
(51) Nymeyer, H.; Woolf, T. B.; Garcia, A. E. *Proteins: Struct. Funct. Bioinf.* **2005**, *59*, 783.
(52) Gorbenko, G. P.; Kinnunen, P. K. J. *Chem. Phys. Lipids.* **2006**, *141*, 72.
(53) Kirkitadze, M. D.; Condron, M. M.; Teplow, D. B. *J. Mol. Biol.* **2001**, *312*, 1103.

JP905889Z